Optical study of thermally annealed Er-doped hydrogenated *a*-Si films

A. R. Zanatta[1] and F. L. Freire, Jr.[2]
[1]Instituto de Física de São Carlos, USP, P.O. Box 369, São Carlos, 13560-250 SP, Brazil
[2]Departamento de Física, PUC-RJ, P.O. Box 38071, Rio de Janeiro, 22452-970 RJ, Brazil
(Received 25 October 1999; revised manuscript received 27 January 2000)

Erbium-doped hydrogenated amorphous silicon (*a*-SiEr:H) films were deposited by co-sputtering a Si target covered with small metallic Er pieces. After deposition the films were submitted to isochronal cumulative thermal anneals in an inert atmosphere of Ar. Rutherford backscattering, Raman spectroscopy, optical transmission, and photoluminescence measurements were employed for characterization purposes. Whereas thermal anneals at temperatures up to ~300 °C do not cause significant changes in the composition, structure, and optical band gap of the present *a*-SiEr:H films, a considerable enhancement of the Er-related light emission at 1540 nm was verified. Thermal treatments at temperatures higher than ~300 °C induce the outdiffusion of hydrogen atoms and consequent increase of structural disorder. Based on these experimental data, and on the available literature, some mechanisms related to the role played by thermal anneals on SiEr compounds are proposed and discussed.

I. INTRODUCTION

Rare-earth (RE) ions when inserted in their trivalent form in solid hosts exhibit atomiclike optical transitions due to their incomplete $4f$ shell. Although parity forbidden in the free ion, these intra-$4f$ transitions are allowed in solids because of mixing of opposite parity states due to the presence of local electric fields in the solid host.[1] As a result of the shielding produced by the filled $5s^2$ and $5p^6$ shells the interaction of the RE ions with the host matrix is feeble and the wavelength of the intra-$4f$ emission depends very weakly on the actual host. As a consequence, RE-doped insulating compounds have been considered for a long time very attractive candidates for lasers sources.[2] Among the various trivalent RE ions, Er^{3+} is the most interesting one since its $^4I_{13/2} \rightarrow ^4I_{15/2}$ transition takes place at 1540 nm, the wavelength at which the transmission loss of the actual silica-based optical fibers is a minimum. In view of their possible application in *photonics*, and taking advantage of the Si technology, Er^{3+} ions have been inserted and studied in several different Si-based compounds. Crystalline (*c*-) and amorphous (*a*-) Si are among the most important hosts and ion implantation is largely employed for the Er insertion.[3] Plasma assisted methods have been chosen for preparing *a*-SiEr compounds by either co-deposition or ion implantation.[3–7] In all of these cases, the attainment of efficient Er-related light emission depends on the presence of impurities and on the thermal annealing treatments. Despite clear indication relative to their influence on the enhancement of the Er luminescence, there is no general agreement on the exact role played by these two procedures. Thermal anneals are mainly associated[8–10] with structural modifications such as: irradiation damage recovery due to ion implantation, atomic diffusion and rearrangement, etc. The presence of impurities is believed to cause:[11–14] a break of the intra-$4f$ selection rules, changes in the local atomic bonding, isolation of the Er^{3+} center, gettering of nonradiative recombination centers, etc. With these ideas in mind and, in order to investigate the influence of thermal anneals on SiEr compounds, this paper presents a systematic study of a series of co-deposited Er-doped *a*-Si:H films.

II. EXPERIMENT

The Er-doped *a*-Si:H film was prepared by rf sputtering from a 5 in. diameter Si target partially covered with small metallic Er platelets. During deposition, a mixture of ultrahigh-purity Ar (5×10^{-4} Torr) and H_2 (5×10^{-4} Torr) gases, and a rf power density of ~0.85 W cm^{-2} were employed. The *a*-SiEr:H film was prepared at room temperature (RT) on both polished *c*-Si and soda-lime glass substrates at the same deposition run. After deposition, the film and respective substrates were divided in several pieces and submitted to cumulative thermal anneals (TA's) in a quartz tube furnace under a continuous gas flow of dry Ar. TA treatments took place at predefined temperatures ($T_a \pm 25$ °C) and were 15 min long. Details concerning all optical measurements and respective data processing can be found elsewhere.[5,10] Rutherford backscattering (RBS) was performed using a 2-MeV He^+ beam, provided by a 4 MV Van de Graaff accelerator. The incidence was normal and the surface-barrier detector was positioned at 165°.

III. EXPERIMENTAL RESULTS

Most of the features observed in an *a*-semiconductor results from its previous history. To the deposition method is attributed the amorphous or disorganized atomic pattern of the film as well as its final composition. As a consequence, every single property of an *a*-film is associated with both the atomic arrangement and relative concentration. Moreover, postdeposition sample modifications by means of energetic processes such as thermal treatments, for example, act as modifying agents and deserve special attention. In this respect, and to achieve a good description of the phenomena taking place in the thermally annealed *a*-SiEr:H film, several different experimental techniques were applied.

The relative concentrations of Er, Ar, Si, and O were

0163-1829/2000/62(3)/2016(5)/$15.00 PRB 62 ©2000 The American Physical Society

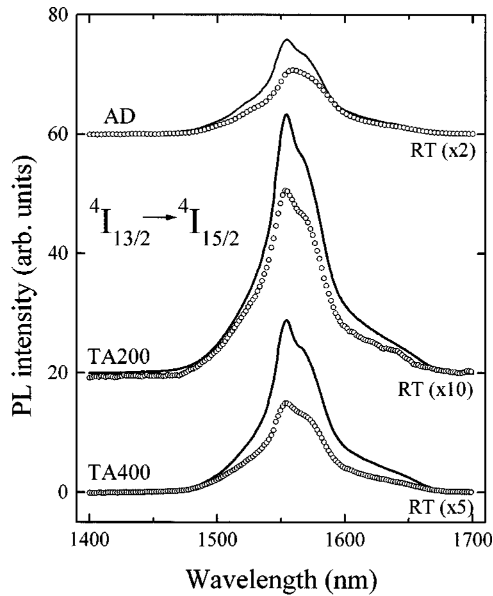

FIG. 1. Photoluminescence spectra of Er-doped a-Si:H films, as-deposited (AD) and thermally annealed at 200 °C (TA200) and 400 °C (TA400). The signals observed at 1540 nm correspond to the $^4I_{13/2} \rightarrow ^4I_{15/2}$ transition characteristic of Er^{3+} ions. The lines correspond to measurements taken at 77 K and the open circles to those obtained at room temperature. Notice the multiplying factors applied to the spectra obtained at room temperature. The spectra have been vertically shifted for clarity.

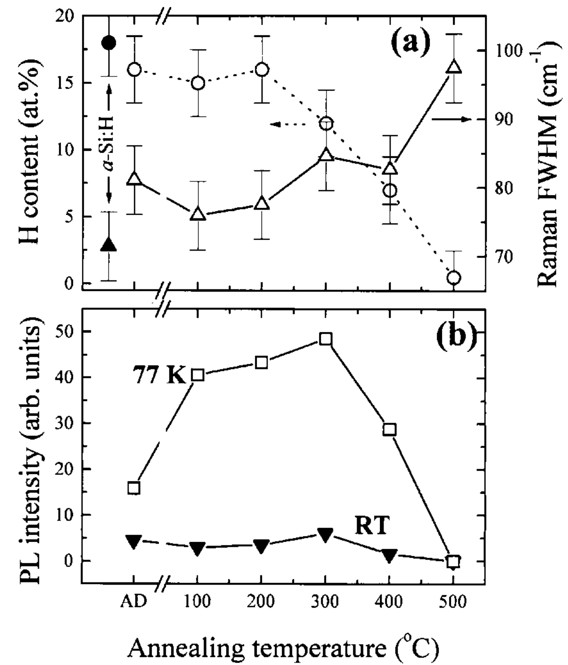

FIG. 2. (a) Hydrogen atomic concentration and the Raman FWHM as a function of the annealing temperature. (b) Er-related PL intensity due to the $^4I_{13/2} \rightarrow ^4I_{15/2}$ transition at ~1540 nm obtained from measurements at room temperature and at 77 K. The data indicated by a-Si:H correspond to pure hydrogenated amorphous silicon films deposited under very similar conditions. The lines are guides to the eye. AD stands for as-deposited samples.

achieved from RBS by simulating the experimental spectra with the RUMP code.[15] The hydrogen content, on the other hand, was obtained from the Si–H absorption bands in the infrared region with the help of appropriate proportionality constants.[10] The Raman spectra of all films exhibit a broad scattering signal at ~480 cm^{-1}, which is a characteristic feature of a-Si matrices. Besides, it is important to emphasize the absence of contributions due to c-Si at ~520 cm^{-1}, even for films treated up to 500 °C.[5]

Figure 1 displays the PL spectra of some a-SiEr:H samples in the ~1400–1700-nm wavelength range both at RT and at 77 K. According to the figure, the most intense PL signal occurs for the film treated near 200 °C. Except for their signal intensities, all films exhibit the same features with a well-pronounced emission at ~1540 nm that corresponds to the $^4I_{13/2} \rightarrow ^4I_{15/2}$ Er^{3+} transition.[1]

IV. DISCUSSION

The overall effect of thermal treatments on the composition, structure, and optoelectronic properties of the present Er-doped a-Si:H films can be appreciated in Fig. 2.[16] Where applicable, the data corresponding to a pure a-Si:H film (deposited under very similar conditions, in the same deposition setup) were displayed for comparison.

A. Composition, structure and optoelectronic properties of Er-doped a-Si:H films

The hydrogen content [H], Raman data, and photoluminescence (PL) intensity as a function of the annealing temperature are shown in Fig. 2. As can be seen from Fig. 2(a), there is a substantial decrease in [H] for films treated at temperatures higher than ~300 °C. The Er concentration, on the other hand, remained at around 0.5 at. % for the whole series. Analogously, the content of occluded Ar, as a consequence of the deposition by rf sputtering in an Ar atmosphere, was ~5 at. %. Concerning the content of oxygen in the a-SiEr:H films, and taking into account the sensitivity of our RBS measurements, it is important to emphasize that [O] <1 at. %.

While optical processes in c-semiconductors are subjected to crystal momentum and symmetry selection rules, the only rule taking place in a-semiconductors is the conservation of energy. As a consequence, it is well established that the tetrahedral short-range order is nearly preserved in a-matrices, and the density of vibrational states of these materials is a broadened version of that of their crystalline counterpart. Besides, changes in the full width at half maximum (FWHM) height of the transverse-optical vibration mode correspond to modifications in the short-range order, particularly in the bond-angle distribution.[17] In this respect, the relationship between the Raman FWHM and structural disorder is well founded and extensively employed as an important characteristic of a-semiconductors.[18] The Raman FWHM values of the present films were obtained from a Gaussian function adjusted to the high-wave number side of the Raman signal at ~480 cm^{-1}. These Raman FWHM values are presented in Fig. 2(a) as a function of the annealing temperature (T_a). The Raman FWHM value of a pure a-Si:H film deposited under very similar conditions, was also displayed for comparison. According to Fig. 2(a), the introduction of Er in the a-Si:H host causes an increase of ~10 cm^{-1} in the Raman FWHM. That value remains practically constant up to

~300 °C and presents a systematic increase at higher temperatures. Taking into account the beneficial effect of H atoms in saturating dangling bonds in *a*-semiconductors,[19] a high density of defects is expected in the mobility gap of *a*-SiEr:H films with a hydrogen concentration lower than ~5 at. %. The outdiffusion of hydrogen and the consequent increase of structural disorder are in agreement with the Raman FWHM values [Fig. 2(a)].

Hydrogen outdiffusion, and the consequent creation of defects, can be associated with the PL results pointing out the dependence of the Er-related light emission at ~1540 nm with the occurrence of nonradiative processes. According to Fig. 2(b), the Er-related PL intensity (I_{PL}) increases in the temperature range as-deposited (AD)$\leq T_a \leq$300 °C, where the hydrogen content and Raman FWHM values remain practically constant. Within this temperature range, it is possible that thermal treatments induce a partial atomic reordering (not detected by Raman experiments)[18] and/or the diffusion of light impurities in the *a*-network. At increasing T_a's (>300 °C) the hydrogen concentration is significantly reduced and a decrease in the Er-related PL intensity is indeed verified. At this point it is important to stress that, in contrast to the hydrogen content and the Raman FWHM signal, neither the Er concentration nor the optical band gap (not shown) have changed remarkably. As a consequence, the decrease of the Er-related PL for T_a>300 °C is determined by nonradiative losses due to defects in the *a*-SiEr:H films.

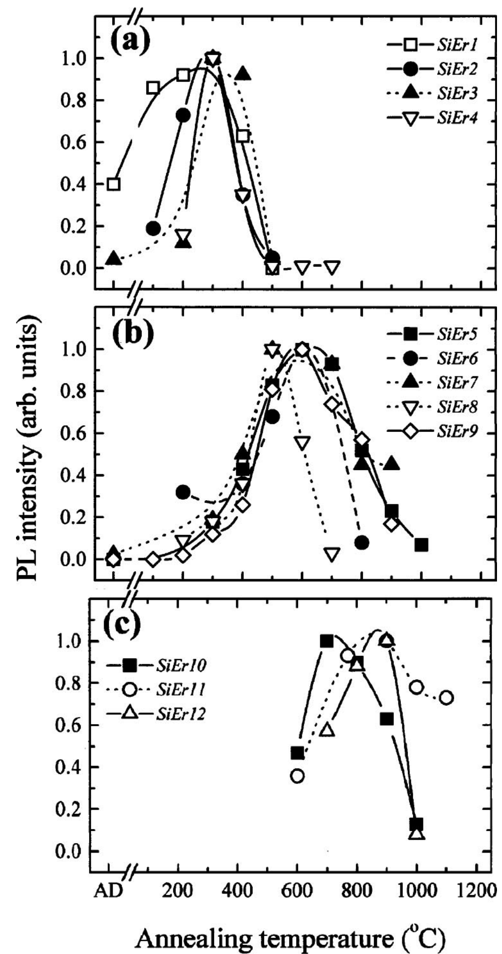

FIG. 3. Er-related PL intensity as a function of the annealing temperature for several different Er-doped Si-based compounds. All experimental data had their maximum values normalized for comparison purposes. According to the figure and, depending on the samples characteristics, at least three different classes of samples could be identified. (a) *Hydrogen-related*, corresponding to amorphous SiEr samples prepared at relatively low temperatures and with a concentration of impurities (mainly oxygen) bellow ~2 at. %. [***SiEr1*** (this work), ***SiEr2*** (Ref. 20), ***SiEr3*** (Ref. 21), ***SiEr4*** (Ref. 6)]. (b) *Impurity-rich*, corresponding to either amorphous (obtained at temperatures higher than ~200 °C) or crystalline SiEr samples, and with a concentration of impurities higher than ~3 at. % [***SiEr5*** (Ref. 8), ***SiEr6*** (Ref. 22), ***SiEr7*** (Ref. 23), ***SiEr8*** (Ref. 5), ***SiEr9*** (Ref. 24)]. (c) *Crystal-like* SiEr samples with [O] ~1 at. %. [***SiEr10*** (Ref. 9), ***SiEr11*** (Ref. 12), ***SiEr12*** (Ref. 14)]. The lines are guides to the eye.

B. Er-related PL intensity versus annealing temperature

The belllike shape exhibited by I_{PL} versus T_a [Fig. 2(b)] is typical of most of the Er-doped Si-based compounds. While thermal anneals up to ~300 °C seem to be the best ones for the achievement of the most intense Er-related PL signal in the present *a*-SiEr:H films, that temperature will depend very much on the sample details: if crystalline or not, if implanted or codeposited, if free of impurities like oxygen or not, etc. In this respect, Fig. 3 displays the I_{PL} versus T_a experimental data of several Er-doped Si materials as obtained from the literature. The figure contains data from distinct authors and from quite different Er-doped samples, and have been grouped based on their main characteristics. The labels of Fig. 3 correspond to: ***SiEr1*** (this work), ***SiEr2*** (Er-doped *a*-Si:H film codeposited at RT),[20] ***SiEr3*** (Er-implanted *a*-Si:H with [O]~1.3 at. %),[21] ***SiEr4*** (Er-doped *a*-Si:H codeposited at 200 °C),[6] **SiEr5** (Er-implanted *semi-insulating polycrystalline Si* SIPOS with [O]~31 at. %),[8] ***SiEr6*** (Er- and N-doped *a*-Si:H codeposited at 200 °C with [N]~5 at. %),[22] ***SiEr7*** (Er-implanted SIPOS with [O] ~27 at. %),[23] ***SiEr8*** (Er-doped *a*-Si:H codeposited at 220 °C and with [O]~3 at. %),[5] ***SiEr9*** (Er-doped *a*-SiO coevaporated),[24] ***SiEr10*** (Er-implanted *oxygen-doped* Si *epitaxial* films OXSEF with [O]~10 at. %),[9] ***SiEr11*** (Er-implanted *Czochralski*-grown CZ Si wafers with [O]~5 $\times 10^{18}$ cm^{-3}),[12] and ***SiEr12*** (Er-implanted CZ Si with [O] ~2$\times 10^{18}$ cm^{-3}).[14]

Taking into account the main characteristics of each series of samples, and excluding fine details associated with the annealing procedures (time of anneal, if cumulative or not, preannealing steps, etc.), the maximum I_{PL} occurs at three different ranges of temperature that have been classified as:

(i) *Hydrogen-related* films [Fig. 3(a)]: have the maximum I_{PL} in the 200 °C$\leq T_a \leq$400 °C range and correspond to Er-doped *a*-Si:H samples deposited at room or relatively low temperatures ($\leq$200 °C). While [H]~10–20 at. % in the as-deposited samples, their typical impurity content (mainly oxygen) stays below ~2 at. %. The assignment of these films as *hydrogen-related* originate from their strong dependence on [H].

(ii) *Impurity-rich* films [Fig. 3(b)]: have the maximum I_{PL} in the 500 °C$\leq T_a \leq$700 °C range and correspond to either amorphous (deposited at temperatures higher than 200 °C) or

crystalline SiEr samples. The designation as *impurity-rich* films comes from their typical impurity content (either oxygen or nitrogen) which is, necessarily, higher than ~3 at.%.

(iii) *Crystal-like* samples [Fig. 3(c)]: have the maximum I_{PL} in the $700\,^\circ C \leqslant T_a \leqslant 900\,^\circ C$ range and correspond to Er-implanted crystalline Si samples. For these samples, the oxygen content usually stays around ~1 at.%. Despite the crystalline character of the Si host, there should be some lattice distortion around the Er ions after implantation. Moreover, and to the best of our knowledge, there is no direct evidence endorsing the crystal quality of these ion implanted *c*-Si wafers. As a consequence, they have been identified as *crystal-like*.

Based on the above classification it is possible to suggest, at least, two different mechanisms imposed by the thermal treatments that dictate the observed I_{PL} behavior.

(a) The first one, before the attainment of the maximum Er-related PL intensity, is associated either with the diffusion of light atoms or with the damage recovery after the ion implantation process. Whereas atomic diffusion takes place in *hydrogen-related* and *impurity-rich* films, the damage recovery after ion implantation occurs in *crystal-like* samples. Strictly speaking, the atomic diffusion in the Si matrix is responsible for the passivation of defects with hydrogen or other light impurities such as oxygen, nitrogen, etc. In such a case, the optimum temperature (when the maximum I_{PL} is achieved) will be determined by both structural and chemical aspects of the Si matrix (Fig. 3). Atomic diffusion and/or energetic reactions can also promote the formation of Er complexes such as Si-impurity[25] and give rise to the observed I_{PL} improvement. The diffusion of atoms and creation of Er complexes, however, cannot be completely discarded in the *crystal-like* samples and certainly influence their overall I_{PL} behavior. In all cases, at maximum I_{PL}, the number of active Er^{3+} centers fairly exceeds the nonradiative ones.

(b) The second mechanism, after the maximum I_{PL} has been reached, again involves a competition between the radiative recombination of Er^{3+} ions and nonradiative losses (mainly due to defects). At this point, however, the rate of defect formation is remarkably high causing a considerable decrease in the Er-related PL signal. Under this regime, the outdiffusion of hydrogen atoms and the consequent increase in the number of dangling bonds is predominant in the *hydrogen-related* films. A similar process of atomic outdiffusion, but at higher temperatures (based on chemical considerations), occurs in the *impurity-rich* films. The creation of nonradiative centers (or defects) is also at the origin of the Er-related PL decrease in the *crystal-like* samples after the maximum I_{PL} has been reached. Moreover, it is convenient to point out that, depending on the temperature of anneal, part of these new nonradiative paths originate from the breakup of some Si-impurity complexes.

A third process can also be suggested in view of the experimental results of Fig. 3 and takes place at the highest T_a temperatures, when I_{PL} approaches zero. In such a case, either due to atomic outdiffusion or due to the break of Er complexes, the number of nonradiative centers in the Si matrix is very high and extinguishes the radiative recombination via Er^{3+} ions.

IV. SUMMARY

Er-doped hydrogenated amorphous silicon *a*-SiEr:H films were deposited by cosputtering. After deposition the films were submitted to cumulative thermal anneals in an inert atmosphere and investigated through RBS, Raman spectroscopy, optical transmission, and PL measurements. According to the experimental results, thermal anneals at temperatures up to ~300 °C do not cause significant changes on the composition and structure of the present *a*-SiEr:H films. Within this temperature range, however, a considerable enhancement of the Er-related PL intensity at ~1540 nm was verified. Thermal treatments at temperatures higher than ~300 °C induce the outdiffusion of hydrogen atoms and consequent increase of structural disorder. In view of these experimental data, and based on the existing literature, three different classes of SiEr samples were proposed. Following their main structural and compositional characteristics they were identified by *hydrogen-related, impurity-rich*, and *crystal-like* samples. Moreover, based on the distinctive I_{PL} versus T_a behavior of these three classes of samples, some mechanisms related to the role played by thermal anneals were proposed and discussed. Before the attainment of the maximum Er-related PL intensity, thermal anneals induce either atomic diffusion in *hydrogen-related* and *impurity-rich* films or the damage recovery due to ion implantation in the *crystal-like* samples. After the maximum Er-related PL intensity, thermal anneals at increasing temperatures promote the formation of defects and a consequent reduction of the Er-related PL signal.

ACKNOWLEDGMENTS

This work was supported by the Brazilian Agencies FAPESP and CNPq. PL and Raman characterization have been performed at the Laboratory of Optical Spectroscopy (USP).

[1] G. H. Dieke, *Spectra and Energy Levels of Rare Earth Ions in Crystals* (Wiley Interscience, New York, 1968).

[2] See, for instance, J. Wilson and J. F. B. Hawkes, *Lasers–Principles and Applications* (Prentice Hall, London, 1987).

[3] A. Polman, J. Appl. Phys. **82**, 1 (1997), and references therein.

[4] M. S. Bressler, O. B. Gusev, V. Kh. Kudoyarova, A. N. Kuznetsov, P. E. Pak, E. I. Terukov, I. N. Iassievich, B. P. Zakharchenya, W. Fuhs, and A. Sturm, Appl. Phys. Lett. **67**, 3599 (1995).

[5] A. R. Zanatta, L. A. O. Nunes, and L. R. Tessler, Appl. Phys. Lett. **70**, 511 (1997).

[6] A. A. Andreev, V. B. Voronkov, V. G. Golubev, A. V. Medvedev, and A. B. Pevtsov, Semiconductors **33**, 93 (1999).

[7] T. Oestereich, C. Swiatowski, and I. Broser, Appl. Phys. Lett. **56**, 446 (1990).

[8] G. N. van den Hoven, J. H. Shin, A. Polman, S. Lombardo, and S. U. Campisano, J. Appl. Phys. **78**, 2642 (1995).

[9] R. Serna, E. Snoeks, G. N. van den Hoven, and A. Polman, J. Appl. Phys. **75**, 2644 (1994).

[10] A. R. Zanatta and L. A. O. Nunes, Appl. Phys. Lett. **71**, 3679 (1997).

[11] D. L. Adler, D. C. Jacobson, D. J. Eaglesham, M. A. Marcus, J. L. Benton, J. M. Poate, and P. H. Citrin, Appl. Phys. Lett. **61**, 2181 (1992).

[12] J. Michel, J. L. Benton, R. F. Ferrante, D. C. Jacobson, D. J. Eaglesham, E. A. Fitzgerald, Y.-H. Xie, J. M. Poate, and L. C. Kimmerling, J. Appl. Phys. **70**, 2672 (1991).

[13] F. G. Anderson, Appl. Phys. Lett. **68**, 2421 (1996).

[14] H. Przybylinska, W. Jantsch, Y. Belevitch, M. Stepikhova, L. Palmetshofer, G. Hendorfer, A. Kozanecki, R. J. Wilson, and B. J. Sealy, Phys. Rev. B **54**, 2532 (1996).

[15] L. R. Doolittle, Nucl. Instrum. Methods Phys. Res. B **9**, 344 (1985).

[16] While all deposition runs started at RT it is important to emphasize that, after the first hour, that temperature can be as high as 50 °C. For such a reason, AD corresponds to as-deposited films (with no thermal anneal) and were inserted in Fig. 2 by means of an axis break.

[17] J. S. Lannin, in *Semiconductors and Semimetals*, edited by J. I. Pankove (Academic, New York, 1984), Vol. 21B, p. 159.

[18] A. R. Zanatta, M. Mulato, and I. Chambouleyron, J. Appl. Phys. **84**, 5184 (1998), and references therein.

[19] See, for instance, R. A. Street, *Hydrogenated Amorphous Silicon* (Cambridge University Press, Cambridge, 1992).

[20] E. I. Terukov, O. I. Kon'kov, V. K. Kudoyarova, O. B. Gusev, G. Weiser, and H. Kuehne, Semiconductors **33**, 177 (1999).

[21] J. H. Shin, R. Serna, G. N. van den Hoven, A. Polman, W. G. J. H. M. van Sark, and A. M. Vredenberg, Appl. Phys. Lett. **68**, 997 (1996).

[22] A. R. Zanatta and L. A. O. Nunes, J. Non-Cryst. Solids **227–230**, 389 (1998).

[23] S. Lombardo, S. U. Campisano, G. N. van den Hoven, A. Cacciato, and A. Polman, Appl. Phys. Lett. **63**, 1942 (1993).

[24] S. W. Roberts and G. J. Parker, Electron. Lett. **31**, 1499 (1995).

[25] See, for example, V. F. Masterov, F. S. Nasredinov, P. P. Seregin, V. K. Kudoyanova, A. N. Kuznetsov, and E. I. Terukov, Appl. Phys. Lett. **72**, 728 (1998).